

1 This is the author's accepted manuscript. The final published version of this work (the version of record)
2 is published by Elsevier in *Science of the Total Environment*. The accepted manuscript was made
3 available online on the 15 July 2019 at: <https://doi.org/10.1016/j.scitotenv.2019.07.041> This work is
4 made available online in accordance with the publisher's policies. Please refer to any applicable terms of
5 use of the publisher.

7 **Biomonitoring acidification using marine gastropods**

8
9 David J. Marshall^{1*}, Ahmed Awad Abdelhady², Dennis Ting Teck Wah¹, Nurshahida
10 Mustapha¹, Stefan H. Gödeke³, Liyanage Chandratilak De Silva⁴, Jason M. Hall-Spencer^{5,6}

11
12 ¹Environmental and Life Sciences, Faculty of Science, Universiti Brunei Darussalam, Brunei
13 Darussalam; ²Geology Department, Faculty of Science, Minia University, El-Minia 61519,
14 Egypt; ³Geological Sciences, Faculty of Science, Universiti Brunei Darussalam; ⁴Faculty of
15 Integrated Technologies, Universiti Brunei Darussalam; ⁵School of Biological and Marine
16 Sciences, University of Plymouth, UK; ⁶ Shimoda Marine Research Center, Tsukuba
17 University, Japan.

18
19 *Corresponding author: David J. Marshall, Environmental and Life Sciences, Faculty of
20 Science, Universiti Brunei Darussalam, Jalan Tungku Link, BE1410, Gadong, Brunei
21 Darussalam. Email: david.marshall@ubd.edu.bn; Tel.: +673 8974143

30

31

32

33 **Abstract**

34 Ocean acidification is mainly being monitored using data loggers which currently offer limited
35 coverage of marine ecosystems. Here, we trial the use of gastropod shells to monitor
36 acidification on rocky shores. Animals living in areas with highly variable pH (8.6 - 5.9) were
37 compared with those from sites with more stable pH (8.6 - 7.9). Differences in site pH were
38 reflected in size, shape and erosion patterns in *Nerita chamaeleon* and *Planaxis sulcatus*. Shells
39 from acidified sites were shorter, more globular and more eroded, with both of these species
40 proving to be similarly good biomonitors. After an assessment of baseline weathering, shell
41 erosion can be used to indicate the level of exposure of organisms to corrosive water, providing
42 a tool for biomonitoring acidification in heterogeneous intertidal systems. A shell erosion
43 ranking system was found to unequivocally discriminate between acidified and reference sites.
44 Being spatially-extensive, this approach can identify coastal areas of greater or lesser
45 acidification. Cost-effective and simple shell erosion ranking is amenable to citizen science
46 projects and could serve as an early-warning-signal for natural or anthropogenic acidification
47 of coastal waters.

48 **Keywords:** ocean acidification; bioindicators; acid sulphate soils; calcification; snails;
49 tropical

50 **1. Introduction**

51 Monitoring changes in the corrosiveness of seawater is crucial to managing and predicting the
52 impact of ocean acidification. The past two decades have seen an increase in the global
53 deployment of fixed buoys equipped with instruments and data-loggers. These monitoring
54 stations capture long-term changes in seawater chemistry but are costly to implement and
55 maintain, and provide data from discrete points. Biomonitoring may provide a complementary
56 method for assessing acidification in coastal waters. Shelled gastropods can be useful
57 biomonitoring organisms (Gibbs et al., 1987; Phillips and Rainbow, 1993; Zhou et al., 2008;
58 Nuñez et al., 2012, Márquez et al., 2015; Proum et al., 2016; Begliomini et al., 2017) and so
59 oceanographers have begun to use pteropod shell dissolution to assess the effects of
60 acidification in the open sea (Bednaršek et al., 2012a, 2012b, 2014). Here, we propose an

61 approach using benthic gastropods to assess acidification impacts in shallow-water coastal
62 habitats.

63 Studies of benthic gastropods have contributed significantly to our understanding of the
64 ecological consequences of ocean acidification (Lardies et al., 2014; Garilli et al., 2015). Much
65 of this work has focussed on the energetic costs of calcification in acidified water (Chen et al.,
66 2015; Harvey et al., 2016, 2018; Connell et al., 2017; Duquette et al., 2017; Doubleday et al.,
67 2017; Harvey et al., 2018). Gastropod shell mineralogy, dissolution and gross shell deformities
68 are well documented, especially for CO₂ seep systems (Hall-Spencer et al., 2008; Chen et al.,
69 2015; Duquette et al., 2017), yet no studies have assessed how well these features record
70 episodes when seawater becomes corrosive to shells and skeletons.

71 Fluctuations in carbonate chemistry in near-shore marine environments arise from multiple
72 natural and anthropogenic processes, with a major influence from the land via rivers, estuaries
73 and sediments (Zhai et al., 2015). Carbonate undersaturation in coastal waters can be caused
74 by flooding and reduced salinities, or eutrophication (Cai et al., 2011 a, b; Duarte et al., 2013;
75 Zhai et al., 2015). Coastal acidification also develops through geochemical discharge from
76 acidic soils (Powell and Martens, 2005; Grealish and Fitzpatrick, 2013). In Brunei (Borneo,
77 South East Asia), a combination of eutrophication, peat swamp leachate, acidic pollutants and
78 acid sulphate soils cause coastal acidification (Marshall et al., 2008; Grealish and Fitzpatrick,
79 2013; Proum et al., 2016, 2018), reducing biodiversity and affecting ecosystem functions
80 (Marshall et al., 2016, 2018). A steep pH gradient in the Brunei estuarine system has been used
81 to assess marine organism and community responses to acidification (Bolhuis et al., 2014;
82 Hossain and Marshall, 2014; Majewska et al., 2017; Proum et al., 2017).

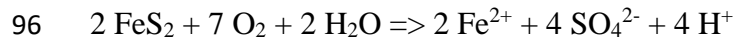
83 Gastropod snails with heavily corroded shells inhabit the rocky intertidal zone on the open
84 coast of Brunei, away from influence of the estuarine system. Here we investigated the effect
85 of acidic water discharge on rocky shore seawater pH. We then tested whether gastropods can
86 be used to inform about corrosive water conditions on rocky shores, by comparing between
87 responses to acidified and normal seawater exposure using two species. An overarching
88 objective was to appraise methods using shells of benthic gastropods to monitor corrosive
89 seawater events.

90

91 **2. Materials and Methods**

92 2.1 Geology and study sites

93 The South China Sea coast of Brunei Darussalam has sandstone ridges separated by clay
94 sediments containing pyrite (FeS₂) and pyritic minerals (Morley et al., 2003) which react when
95 exposed to oxygen according to the equation:



97 This lowers the pH of water that flows from the land into the South China Sea (Grealish and
98 Fitzpatrick, 2013) (Fig. 1). Water enters the coastal ecosystem via tributaries and watercourses,
99 or through discharges of submarine or subterranean groundwater, which can be below pH 4
100 (Azhar et al., 2019; Waska et al., 2019; Fig. 1). Topography, tides, currents and waves influence
101 the area of seawater affected by groundwater discharge (Urish and McKenna, 2004; Waska et
102 al., 2019).

103 Eight sites were selected based on the occurrence of *Nerita chamaeleon* Linnaeus, 1758
104 (Neritoidea) and *Planaxis sulcatus* (Born, 1778) (Cerithioidea) and on the presence of intertidal
105 acidic water discharge (Fig. 1). Three sites were strongly influenced by acidified water (E1, E2
106 and E3; A1) whereas the reference sites were not (JPMC, PJER, PUN, TP, UB). PUN and E1-
107 3 were natural rocky shores, whereas the others were artificial seawalls (Fig. 1, A1). At low
108 tide E1-3 had acidified water running over mixed sand and boulders exposing both species of
109 gastropod to acidified water although when the tide was in, seawater pH and salinity were
110 normal (Grealish and Fitzpatrick, 2013; A1). Sites were separated by km scale distances, except
111 E1-3 which were approximately > 100 m apart. Physicochemical characteristics, such as
112 temperature and oxygen content, were similar across the sites.

113 2.2 Sampling

114 A total of 124 water samples (40 ml, between 9-32 per site) were collected from snail habitat
115 in the intertidal zone on thirteen trips in April-July 2018. Samples were taken to measure pH
116 and salinity ranges during low-tide, including from small pools on the high shore, and from the
117 open sea on the low shore. Sometimes small water-bodies were sampled with a syringe. On
118 return to the laboratory, water parameters were measured at 24°C, the laboratory and night-
119 time field temperature. Salinity was measured using a Hach multi-meter (model HQ40d) with
120 an Intellical probe (Hach Lange GmbH Headquarter, Düsseldorf, Germany). pH was measured
121 using a Mettler Toledo pH transmitter 2100e and probe (Mettler-Toledo GmbH, Giessen,
122 Germany) calibrated with pH 4.00 and 7.00 CertiPUR Merk buffers traceable to SRM from

123 NIST. Repeated measures of the same sample yielded a reading precision of
124 ± 0.012 (s. d., $n = 10$).

125 *Nerita chamaeleon* and *P. sulcatus* are common on rocky-shores in this region of Asia.
126 Individuals of both species occupy hard-substrata, intertidal pools, and sometimes soft
127 sediments between boulders, across a broad mid-tidal zone (approximately 0.5-1.5 m Chart
128 Datum). Abundance in both cases can exceed 50 snails per m^2 . The species differ greatly in
129 shell shape with the shell of *N. chamaeleon* expanded diametrical and compressed axially and
130 that of *P. sulcatus* expanded axially (Figs. 2 and 3). Similar-sized living adults (20-30 mm for
131 both species) were collected and analysed between Dec 2016 and Jul 2018. Snails of *N.*
132 *chamaeleon* ($n = 132$) and *P. sulcatus* ($n = 147$) were stored in 70% ethanol within an hour of
133 collection. Shell size, shape and surface erosion were then measured or ranked.

134 We compared between the reference and acidified sites using attributes of either species. The
135 same attribute was not always determined for both species, with shell shape often dictating the
136 approach followed. For example, it was not feasible to assess shell shape variation using
137 conventional geometric morphometric landmarks in the case of the globular-shaped *Nerita*
138 *chamaeleon*, which has severely compressed spire whorls.

139 *2.3 Size, mass and shell shape*

140 Shell height, aperture length, dry shell mass and dry soft tissue mass were measured for *N.*
141 *chamaeleon* from E1 (acidified) and PUN (reference) (Fig. 1). After photographing apertural
142 and abapertural shell surfaces (Canon EOS 5D, Mark II, 100 mm macrolens), length was
143 measured using Olympus CellSens software (A2). Shells were then cracked open and separated
144 from soft tissues. Following oven-drying at 70°C for three days, the tissue was weighed with a
145 balance accurate to 0.001 g.

146 Shell length and mass data were scaled to a common aperture length (Marshall et al., 2008,
147 A2). As shell morphology varies allometrically, measurements were converted to natural
148 logarithms before fitting ordinary least squares regressions to plots (Sigmaplot ver. 14, Systat
149 Software, Inc., New York, US). The effect of site (PUN and E1) was assessed using
150 Generalized Linear Models for normal distribution with a log-link function (Statistica ver. 12,
151 StatSoft, New York, US).

152 Shell shape analyses of *P. sulcatus* used samples from E2 (acidified), TP and UB (reference),
153 and followed methods described by Abdelhady et al. (2018). Each individual was photographed

154 (> 20 per site) and twenty landmarks of the shell were digitized using the TPSDig Package
155 (<http://life.bio.sunysb.edu/morph/>, Rohlf, 1996; A3). The error associated with capturing 2D
156 image from 3D object was minimized (see Abdelhady, 2016). Generalized Procrustes Analysis
157 was applied to these data using the method of Rohlf and Slice (1990) to ensure that distances
158 among homologous landmarks were minimized such that the resulting data best represented
159 the shape. Procrustes residual data were projected to Detrended Corresponding Analysis
160 (DCA) to arrange the shell shape data on coordinates (see Abdelhady and Fürsich, 2014, 2015).
161 Analysis of Similarities (ANOSIM) was applied to test the null hypothesis that similarities
162 between sites are smaller or equal to similarities within sites. Finally, Thin Plate Spline was
163 used to assess changes in shell shape between specimens (see Zelditch et al., 2012). Statistical
164 analyses were carried out using PAST version 2.17c (Hammer et al., 2001, 2006).

165 *2.4 Shell surface erosion*

166 Shell erosion areas, representing lifetime exposures, were assessed quantitatively or using a
167 ranking system. Two methods were used to quantify erosion areas from photographs of the
168 abapertural side of *N. chamaeleon* collected from PUN (reference) and E1 (acidified) in Dec
169 2016. Our first method involved manually demarcating and calculating planar surface area (2D)
170 of erosion down to the light grey, fine-textured layer using an Olympus CellSens drawing tool
171 (A2). The eroded area was then expressed as a proportion of the total surface area of the shell.
172 Generalized Linear Models for a normal distribution and log-link function (Statistica ver. 12,
173 StatSoft, New York, US) were used to assess the effect of acidification. For each site, we
174 counted the number of individuals showing no erosion as well as those showing eroded surfaces
175 of > 10% of the total area.

176 Inaccuracies in delineation of areas arose when erosion occurred in the fine grooves of shells
177 (A2), so we applied a second method to *N. chamaeleon* shells based on digital pixel analysis.
178 We developed software that used k-mean clustering, which assigns observations to clusters
179 using Mahalanobis distance measures. We grouped our data into background (white colour),
180 eroded shell surfaces (light colour) and unaffected shell surfaces (dark colour). The digital
181 method was then compared with our manual assessment of eroded areas using a linear
182 regression (Statistica ver. 12).

183 Shell Erosion Ranks (SERs) were determined for both species (Figs 2 and 3) using different
184 criteria for pragmatic reasons (shell shape). For *N. chamaeleon*, erosion ranks were based on
185 apical images of the shell. The image was divided into seven sectors, each representing a

186 different shell age (Fig. 2). A 0 – 7 rank, based on the highest numbered sector with > 50%
187 surface erosion was determined for two types of erosion. Type I was deep erosion to
188 homogenous non-pigmented fine-textured shell and Type II was superficial erosion of the outer
189 ‘prismatic’ layer containing slight ridges and pigmented shell. Our analyses were based on
190 either the rank for Type I (0-7) or that for both types summed to give a final rank between 0 –
191 14 (Fig. 2). A shell that was completely covered by periostracum was scored zero. In *P.*
192 *sulcatus*, shell erosion was ranked using abapertural and apertural photographs (see Fig. 3 for
193 details of the abapertural ranking method). Data were statistically analysed using Generalized
194 Linear Models with a probit function for an ordinal multinomial distribution (Statistica ver.
195 12). Median scores and frequency distributions of ranks were plotted.

196 **3. Results**

197 *3.1 Habitat pH and salinity*

198 Upper pH values were similar for all stations (mean max pH \pm s.d. = 8.50 ± 0.08 , n = 6). pH
199 ranges were 8.56 - 7.90 (n = 63) for the reference sites and 8.60 - 5.93 (n = 61) for the acidified
200 sites (Fig. 4). Salinities were 33.2–20.2 for the reference sites and 32.8 - 0.2 for the acidified
201 sites. In a nearby estuary, lower pH and salinity generated through acidic groundwater
202 discharge causes calcite (Ca) and aragonite (Ar) undersaturation, and so snails at our acidified
203 sites (E1-3) are likely to experience corrosive water exposure (Fig. 4, bottom panel).

204 *3.2 Size, mass and shape*

205 Shells of *N. chamaeleon* from the acidified site were shorter than those at the reference site
206 (A4; Wald stat = 12.88, p= 0.0003). Shell and dry tissue mass did not differ significantly
207 between the sites (Wald stat = 3.42, p = 0.064 and Wald stat = 0.15, p = 0.694, respectively;
208 A4). In the shape analysis of *P. sulcatus*, cumulative plots of the average sizes confirmed the
209 suitability of using ~20 specimens with little change in this average when more specimens were
210 added. Reference-site *P. sulcatus* had similar shell shapes whereas the acidified-site specimens
211 had a larger width/height ratio (ANOSIM; p < 0.01; Fig. 5). DCA confirmed that acidified-site
212 snails had shorter shells with larger apertures. Shell shapes were similar for the reference
213 populations, which differed from the acidified population (DC1 versus DC2, Fig. 5). Apertures
214 were rounder (DC1 versus aperture shape; r = 0.44; Fig. 5) and shells were more globular in
215 acidified conditions (DC2 versus shell height; r = - 0.48; Fig. 5).

216 *3.3 Shell surface erosion*

217 Shells from acidified sites were more eroded than those at reference sites (Fig. 6). Differences
218 were found for manually-calculated absolute areas and areas relative to the total shell surface
219 (Fig. 6 A, B, C; $p < 0.001$). The average amount of eroded surface of acidified site snails was
220 $> 40\%$, compared to $< 10\%$ in reference site snails (Fig. 6). Only one acidified site snail had
221 no dissolution (Fig. 6 D).

222 In our digital technique, surface erosion areas were coloured red vs blue for unaffected areas
223 (Fig. 7). Results from our automated approach and our manual calculations were closely
224 correlated ($r = 0.91$; $p < 0.05$; Fig. 7), though the manual method underestimated eroded areas
225 in shell grooves. Due to its simplicity, the automated technique could be used for large sample
226 analysis although visual checks are needed, such as when the colour of eroded shell areas is
227 similar to that of uneroded areas.

228 Shell Erosion Ranks (SERs) indicated much more extensive erosion at the acidified sites (Figs
229 8 and 9). Reference site *N. chamaeleon* had a median SER of 5 whereas snails from acidified
230 sites had a rank of 10. There were however differences within the groups of reference or
231 acidified sites; PUN shells had greater erosion than JPMC and PJER, and E1 and E2 had more
232 erosion than E3 (Fig. 8 A; Table 1). SER frequencies were highly discriminatory in that ranks
233 of 5 and 6 (Type I), representing the most severe erosion, were only found at the acidified sites
234 (Fig. 8 B). These patterns were repeated in *P. sulcatus* with a median erosion rank of ~ 6.5 at
235 the reference sites compared with ~ 9 for the acidified sites (Fig. 9; Table 1). Whereas most of
236 the snails at the acidified sites had erosion ranks > 5 , the highest rank recorded at the reference
237 sites was 4 and none of the snails at the acidified sites ranked 2 or less (Fig. 9 B). High
238 frequencies of the unique highest (or higher) erosion ranks were found at the acidified sites;
239 ranks 5 or 6 for *N. chamaeleon* collectively contributed more than 0.4 of all individuals and
240 rank 5 for *P. sulcatus* contributed around 0.6 of these populations.

241 **4. Discussion**

242 Gastropod shells have been used to monitor spatial patterns of acidification in oceanic pelagic
243 systems (Bednaršek et al., 2012a, 2012b, 2014) but not in coastal ecosystems. We found that
244 acidification of a rocky intertidal system was reflected in the shell attributes of two gastropod
245 species, with shell surface erosion patterns correlating with acidification.

246 Groundwater discharge affected open coast rocky shores of the region, with some rockpools as
247 low as pH 5.9, adding to previous observations of the effects of acidification on the ecology of
248 an estuarine system in Brunei (Marshall et al. 2008, 2016; Bolhuis et al., 2014; Hossain et al.,

249 2014; Majewska et al., 2017; Proum et al., 2017, 2018). Land-to-sea acidification via
250 submarine groundwater flux or water-course infiltration had little effect on pH at the reference
251 sites compared to that of direct discharge at the acidified sites (Urish and McKenna, 2004).
252 Rockpool pH and salinity fell to levels likely to produce carbonate undersaturation (Fig. 3; Kim
253 et al., 2014; Proum et al., 2018).

254

255 Shell length, shape, and erosion varied greatly between the acidified and reference sites,
256 whereas tissue and shell masses were similar (A4). Acidified water exposure does not always
257 cause shell mass reduction in gastropods (Marshall et al., 2008; Lardies et al., 2014; Chen et
258 al., 2015). Shell growth depends on both carbonate saturation of the surrounding water and
259 feeding opportunities (in turn affecting energetic status), whereas dissolution relates solely to
260 the external saturation state. We recorded shell-shortening and more globular-shaped shells in
261 acidified-site populations of *P. sulcatus* (Fig. 5). In these snails there was apical and upper-
262 spire erosion as well broadening of the shell aperture. Basal broadening likely relates to slower
263 growth in the acidified areas.

264 Gastropod shell surface erosion was a sensitive marker of acidification by recording shell loss
265 that was not readily detectable gravimetrically. This finding extends the known benefits of this
266 biomarker of seawater acidity from oceanic and estuarine gastropods (Marshall et al., 2008;
267 Bednaršek et al., 2012a, 2012b, 2014) to rocky shore animals and ecosystems. Our manually-
268 assessed eroded surface area for *N. chamaeleon* correlated with that computed digitally,
269 although the latter was more accurate as it accounted for small eroded areas between shell ribs.
270 Shell erosion ranking sharply distinguished acidified and reference sites. Median scores for *N.*
271 *chamaeleon* from reference sites were half the value of those for acidified sites (Fig. 8), and
272 similar clear distinction was found for *P. sulcatus* (Fig. 9). Frequency distributions show that
273 that the highest erosion ranks only occur in the low pH sites (Figs 8 and 9). The few cases of
274 low erosion ranks at the acidified sites may represent within-shore movement, whereby snails
275 initially inhabiting higher pH water lower on the shore had recently moved into the more
276 acidified higher-shore habitats.

277 Whereas the number of ranks and the value ascribed to each rank are arbitrary, variation in
278 rank frequency across habitats is important. Despite using different approaches to rank shell
279 erosion, both species showed high frequencies of unique highest (or higher) ranks in acidified
280 site populations (> 0.4), suggesting similarity in their acidification biomonitoring potential.

281 Our system can however be tailored to the scope and precision needs of an investigation. For
282 instance, it is possible to get three-dimensional information about erosion, by integrating
283 dissolution areas with shell thickness measurements (Figs 2 and 3). Although we focused on
284 measuring and ranking the areas of eroded shell surfaces, shell erosion could be estimated from
285 a spiral growth line superimposed on apically-viewed shell images (A6). Erosion could be
286 measured in terms of the ratio of the line length between the growing edge and the eroded shell
287 against the entire growth line (A6). Improvements could also involve integrating shell growth
288 rate and mineralogy of the study species with shell erosion measures.

289 **5. Appraisal of the biomonitoring tool**

290 Gastropod shell erosion as a biomonitoring tool has advantages over buoys fitted with loggers.
291 We were able to use benthic gastropods in intertidal habitats and because they are usually slow
292 moving or sedentary (occupying meter-sized areas), they can be used to monitor acidification
293 over a range of spatial scales, from metres to hundreds of kilometres. Sampling across a region
294 allows identification of areas with greater or lesser impacts of acidification. In addition to
295 recording chronic exposure of individuals, this approach to biomonitoring can compare
296 populations over time (see A7). Assessments of shell erosion are cost-effective and simple to
297 execute without requiring meters or instruments, such that this could gain the involvement and
298 benefits of citizen science (Dickinson et al., 2010; Gaston et al., 2018). Moreover, information
299 on acidification experienced by individual organisms using shell erosion ranking can be related
300 to other parameters (mass, age, growth and reproduction) of the same organism in the field.

301

302 There are important considerations when using shell erosion as a biomarker of seawater
303 acidification. Because time is a function of acidified seawater exposure, similar-aged
304 individuals (such as adults) should be used in biomonitoring exercises. Distinguishing shell
305 dissolution from weathering and bioerosion is not trivial (Schönberg et al., 2017). Shells
306 become worn through daily cycles of heating, cooling, wetting and drying which increase with
307 increasing vertical shore height (Underwood, 1979; Denny, 1988). Shell abrasion also
308 increases with more wave action and/or exposure to suspended sediments (Denny, 1988). It is
309 possible to tell the effects of bioerosion and erosion by acidified water apart, with the
310 characteristic pits and burrows of microborers often becoming conspicuous on shells.
311 Weathering, bioerosion and chemical erosion work together in acidified waters and are
312 accelerated if outer protective layers of the shell are lost. This problem can be surpassed by
313 establishing reference sites that show what shells are like in normal conditions as compared to

314 acidified conditions. In any event, gross shell erosion (as indicated by maximum SER values,
315 Figs 8 and 9), shell deformities and corroded shells in juveniles are independently clear signs
316 of acidified water exposure (Hall-Spencer et al., 2008; Marshall et al., 2008, 2016; Harvey et
317 al., 2018). Notably, gross shell erosion follows exposure to undersaturated carbonate
318 conditions irrespective of the processes driving these, thus this biomarker informs about a
319 change in environmental conditions and not the underlying mechanism.

320 Information on the ecology and biology of biomonitor species is crucial (Phillips and Rainbow,
321 1995). Species attributes such as shell size and thickness, mineralogy, growth rate, animal
322 behaviour and distribution are all important considerations. Biomonitoring potential is likely
323 to vary between gastropod species considering that mineralogy intrinsically influences natural
324 weathering. Local abundance and geographical distribution of a species add value to its use as
325 a biomonitor. Our study species are common rocky intertidal inhabitants and can potentially
326 be used to monitor acidification across the vast Central Indo-Pacific ecoregion (Spalding et al.
327 2007; Palomares and Pauly, 2019). The methods we propose nonetheless provide a framework
328 for developing acidification biomonitoring using other gastropod species across a wide
329 spectrum of marine environments.

330 **6. Conclusions**

331 We show that gastropod shells can be used to assess the presence and effects of acidification
332 in nearshore and benthic coastal marine environments. This has advantages over conventional
333 monitoring in heterogeneous intertidal systems and allows the identification of critically-
334 exposed areas. In addition to indicating acidic discharges into coastal ecosystems, such
335 biomonitoring could help assess the extent of anthropogenic ocean acidification. Though some
336 refinement and standardization of protocols is required, gastropods show potential for
337 biomonitoring of acidification in marine ecosystems.

338 **7. Acknowledgments**

339 DJM is funded through the grant UBD/RSCH/1.4/FICBF(b)/2018/016. SG is the recipient of
340 a research grant UBD/CRG#18. JH-S is funded by the International Educational and
341 Research Laboratory Program of the University of Tsukuba. Azmi Aminuddin, Amalina
342 Brahim and David Relex helped collect and photograph snails.

343 **8. Author contributions**

344 DJM conceived the original idea and JH-S further contextualized this; DJM and DTTW devised
345 methods and approaches; DJM and NM collected, photographed and measured snails; LCDS
346 developed the automated segmentation technique; SG provided input on the geology of the
347 area as well as the supplementary figures. AAA undertook geometric morphometric analysis.
348 All authors contributed to preparing and critically commenting on the manuscript.

349 **9. Conflicts of Interest:** The authors declare no conflicts of interest

350 **10. References**

351 Abdelhady, A.A., 2016. Phenotypic differentiation of the Red Sea gastropods in response to
352 the environmental deterioration: geometric morphometric approach. *J. Afr. Earth Sci.* 115,
353 191–202.

354

355 Abdelhady, A.A., Abdelrahman, E., Elewa, A.M.T., Fan, J., Zhang, S., Xiao, J., 2018.
356 Phenotypic plasticity of the gastropod *Melanoides tuberculata* in the Nile Delta: A pollution-
357 induced stabilizing selection. *Mar. Pollut. Bull.* 133, 701–710.
358 <https://doi.org/10.1016/j.marpolbul.2018.06.026>

359

360 Abdelhady, A.A., Fürsich, F.T., 2014. Macroinvertebrate palaeo-communities from the
361 Jurassic succession of Gebel Maghara (Sinai, Egypt). *J. African Earth Sci.* 97, 173–193.
362 <https://doi.org/10.1016/j.jafrearsci.2014.04.019>

363

364 Abdelhady, A.A., Fürsich, F.T., 2015. Sequence architecture of a Jurassic ramp succession
365 from Gebel Maghara (North Sinai, Egypt): Implications for eustasy. *J. Palaeogeogr.* 4, 305–
366 330. <https://doi.org/10.1016/j.jop.2015.08.008>

367

368 Azhar, A.S., Latiff, A.H.A., Lim, L.H., Gödeke, S.H., 2019. Groundwater investigation of a
369 coastal aquifer in Brunei Darussalam using seismic refraction. *Environ. Earth Sci.* 78, 220.
370 <https://doi.org/10.1007/s12665-019-8203-6>

371

372 Bednaršek, N., Feely, R.A., Reum, J.C.P., Peterson, B., Menkel, J., Alin, S.R., Hales, B., 2014.
373 *Limacina helicina* shell dissolution as an indicator of declining habitat suitability owing to
374 ocean acidification in the California Current Ecosystem. *Proc. R. Soc. B Biol. Sci.* 281,
375 20140123–20140123. <https://doi.org/10.1098/rspb.2014.0123>

376

377 Bednaršek, N., Tarling, G.A., Bakker, D.C.E., Fielding, S., Cohen, A., Kuzirian, A., McCorkle,
378 D., Lézé, B., Montagna, R., 2012b. Description and quantification of pteropod shell
379 dissolution: a sensitive bioindicator of ocean acidification. *Glob. Chang. Biol.* 18, 2378–2388.
380 <https://doi.org/10.1111/j.1365-2486.2012.02668.x>

381

382 Bednaršek, N., Tarling, G.A., Bakker, D.C.E., Fielding, S., Jones, E.M., Venables, H.J., Ward,
383 P., Kuzirian, A., Lézé, B., Feely, R.A., Murphy, E.J., 2012a. Extensive dissolution of live
384 pteropods in the Southern Ocean. *Nat. Geosci.* 5, 881–885. <https://doi.org/10.1038/ngeo1635>

385

386 Begliomini, F.N., Maciel, D.C., de Almeida, S.M., Abessa, D.M., Maranhão, L.A., Pereira, C.S.,
387 Yogui, G.T., Zanardi-Lamardo, E., Castro, Í.B., 2017. Shell alterations in limpets as putative
388 biomarkers for multi-impacted coastal areas. *Environ. Pollut.* 226, 494–503.
389 <https://doi.org/10.1016/j.envpol.2017.04.045>

390

391 Bolhuis, H., Schlupe, H., Kristalijn, J., Sulaiman, Z., Marshall, D.J., 2014. Molecular
392 analysis of bacterial diversity in mudflats along the salinity gradient of an acidified tropical
393 Bornean estuary (South East Asia). *Aquat. Biosyst.* 10, 1–13. [https://doi.org/10.1186/2046-](https://doi.org/10.1186/2046-9063-10-10)
394 [9063-10-10](https://doi.org/10.1186/2046-9063-10-10)

395

396 Cai, W.-J., 2011a. Estuarine and coastal ocean carbon paradox: CO₂ sinks or sites of terrestrial
397 carbon incineration? *Ann. Rev. Mar. Sci.* 3, 123–145. [https://doi.org/10.1146/annurev-marine-](https://doi.org/10.1146/annurev-marine-120709-142723)
398 [120709-142723](https://doi.org/10.1146/annurev-marine-120709-142723)

399

400 Cai, W.-J., Hu, X., Huang, W.-J., Murrell, M.C., Lehrter, J.C., Lohrenz, S.E., Chou, W.-C.,
401 Zhai, W., Hollibaugh, J.T., Wang, Y., Zhao, P., Guo, X., Gundersen, K., Dai, M., Gong, G.-
402 C., 2011b. Acidification of subsurface coastal waters enhanced by eutrophication. *Nat. Geosci.*
403 4, 766–770. <https://doi.org/10.1038/ngeo1297>

404

405 Chen, Y.J., Wu, J.Y., Chen, C.T.A., Liu, L.L., 2015. Effects of low-pH stress on shell traits of
406 the dove snail, *Anachis misera*, inhabiting shallow-vent environments off Kueishan Islet,
407 Taiwan. *Biogeosci.* 12, 2631–2639. <https://doi.org/10.5194/bg-12-2631-2015>

408

409 Connell, S.D., Doubleday, Z.A., Hamlyn, S.B., Foster, N.R., Harley, C.D.G., Helmuth, B.,
410 Kelaher, B.P., Nagelkerken, I., Sarà, G., Russell, B.D., 2017. How ocean acidification can
411 benefit calcifiers. *Curr. Biol.* 27, R95–R96. <https://doi.org/10.1016/j.cub.2016.12.004>
412

413 Denny, M., 1988. *Biology and the mechanics of the wave swept environment*. Princeton
414 University Press, New Jersey.
415

416 Dickinson, J.L, Zuckerberg, B., Bonter, D.N., 2010. Citizen science as an ecological research
417 tool: challenges and benefits. *Annu. Rev. Ecol. Syst.* 41, 49-172,
418 <https://doi.org/10.1146/annurev-ecolsys-102209-144636>
419

420 Doubleday, Z.A., Nagelkerken, I., Connell, S.D., 2017. Ocean life breaking rules by building
421 shells in acidic extremes. *Curr. Biol.* 27, R1104–R1106.
422 <https://doi.org/10.1016/j.cub.2017.08.057>
423

424 Duarte, C.M., Hendriks, I.E., Moore, T.S., Olsen, Y.S., Steckbauer, A., Ramajo, L., Carstensen,
425 J., Trotter, J.A., McCulloch, M., 2013. Is ocean acidification an open-ocean syndrome?
426 Understanding anthropogenic impacts on seawater pH. *Estuaries and Coasts* 36, 221–236.
427 <https://doi.org/10.1007/s12237-013-9594-3>
428

429 Duquette, A., McClintock, J.B., Amsler, C.D., Pérez-Huerta, A., Milazzo, M., Hall-Spencer,
430 J.M., 2017. Effects of ocean acidification on the shells of four Mediterranean gastropod species
431 near a CO₂ seep. *Mar. Pollut. Bull.* 124, 917–928.
432 <https://doi.org/10.1016/j.marpolbul.2017.08.007>
433

434 Garilli, V., Rodolfo-Metalpa, R., Scuderi, D., Brusca, L., Parrinello, D., Rastrick, S.P.S.,
435 Foggo, A., Twitchett, R.J., Hall-Spencer, J.M., Milazzo, M., 2015. Physiological advantages
436 of dwarfing in surviving extinctions in high-CO₂ oceans. *Nat. Clim. Chang.* 5, 678–682.
437 <https://doi.org/10.1038/nclimate2616>
438

439 Gaston, K.J., Soga, M., Duffy, J.P., Garrett, J.K., Gaston, S., Cox, D.T.C., 2018. Personalized
440 ecology. *TREE*, 33, 916–925.
441

442 Gibbs, P.E., Bryan, G.W., Pascoe, P.L., Burt, G.R., 1987. The use of the dog-whelk, *Nucella*
443 *lapillus*, as an indicator of tributyltin (TBT) contamination. J. Mar. Biol. Assoc. United
444 Kingdom 67, 507–523. <https://doi.org/10.1017/S0025315400027260>
445

446 Grealish, G.J., Fitzpatrick, R.W., 2013. Acid sulphate soil characterization in Negara Brunei
447 Darussalam: a case study to inform management decisions. Soil Use Manag. 29, 432–444.
448 <https://doi.org/10.1111/sum.12051>
449

450 Hall-Spencer, J.M., Rodolfo-Metalpa, R., Martin, S., Ransome, E., Fine, M., Turner, S.M.,
451 Rowley, S.J., Tedesco, D., Buia, M-C. 2008. Volcanic carbon dioxide vents show ecosystem
452 effects of ocean acidification. doi:10.1038/nature07051
453

454 Hammer, Ø., Harper, D.A.T., Ryan, P.D., 2001. PAST: paleontological statistics software
455 package for education and data analysis. Palaeontol. Electronica 4, 1–9.
456

457 Harvey, B.P., Agostini, S., Wada, S., Inaba, K., Hall-Spencer, J.M., 2018. Dissolution: the
458 Achilles' heel of the Triton shell in an acidifying ocean. Front. Mar. Sci. 5, 1–11.
459 <https://doi.org/10.3389/fmars.2018.00371>
460

461 Harvey, B.P., McKeown, N.J., Rastrick, S.P.S., Bertolini, C., Foggo, A., Graham, H., Hall-
462 Spencer, J.M., Milazzo, M., Shaw, P.W., Small, D.P., Moore, P.J., 2016. Individual and
463 population-level responses to ocean acidification. Sci. Rep. 6, 20194.
464 <https://doi.org/10.1038/srep20194>
465

466 Hossain, M.B., Marshall, D.J., 2014. Benthic infaunal community structuring in an acidified
467 tropical estuarine system. Aquat. Biosyst. 10, 11. <https://doi.org/10.1186/2046-9063-10-11>
468

469 Hossain, M.B., Marshall, D.J., Venkatramanan, S., 2014. Sediment granulometry and organic
470 matter content in the intertidal zone of the Sungai Brunei estuarine system, northwest coast of
471 Borneo. Carpathian J. Earth Environ. Sci. 9, 231–239.
472

473 Lardies, M.A., Arias, M.B., Poupin, M.J., Manríquez, P.H., Torres, R., Vargas, C.A., Navarro,
474 J.M., Lagos, N.A., 2014. Differential response to ocean acidification in physiological traits of

475 *Concholepas concholepas* populations. J. Sea Res. 90, 127–134.
476 <https://doi.org/10.1016/j.seares.2014.03.010>
477

478 Majewska, R., Adam, A., Mohammad-Noor, N., Convey, P., De Stefano, M., Marshall, D.J.,
479 2017. Spatio-temporal variation in phytoplankton communities along a salinity and pH gradient
480 in a tropical estuary (Brunei, Borneo, South East Asia). Trop. Ecol. 58, 251–269.
481

482 Marshall, D.J., Aminuddin, A., Ahmad, S., 2018. Gastropod diversity at Pulau Punyit and the
483 nearby shoreline - a reflection of Brunei's vulnerable rocky intertidal communities. Sci.
484 Bruneiana 17, 34–40.
485

486 Marshall, D.J., Proum, S., Hossain, M.B., Adam, A., Hoon Lim, L., Santos, J.H., 2016.
487 Ecological responses to fluctuating and extreme marine acidification: lessons from a tropical
488 estuary (the Brunei Estuarine System). Sci. Bruneiana Special Is, 1–12.
489

490 Marshall, D.J., Santos, J.H., Leung, K.M.Y., Chak, W.H., 2008. Correlations between
491 gastropod shell dissolution and water chemical properties in a tropical estuary. Mar. Environ.
492 Res. 66, 422–429. <https://doi.org/10.1016/j.marenvres.2008.07.003>
493

494 Márquez, F., Nieto Vilela, R.A., Lozada, M., Bigatti, G., 2015. Morphological and behavioral
495 differences in the gastropod *Trophon geversianus* associated to distinct environmental
496 conditions, as revealed by a multidisciplinary approach. J. Sea Res. 95, 239–247.
497 <https://doi.org/10.1016/j.seares.2014.05.002>
498

499 Morley, C.K., Back, S., Van Rensbergen, P., Crevello, P., Lambiase, J.J., 2003. Characteristics
500 of repeated, detached, Miocene–Pliocene tectonic inversion events, in a large delta province
501 on an active margin, Brunei Darussalam, Borneo. J. Struct. Geol. 25, 1147–1169.
502 [https://doi.org/10.1016/S0191-8141\(02\)00130-x](https://doi.org/10.1016/S0191-8141(02)00130-x)
503

504 Nuñez, J.D., Laitano, M. V., Cledón, M., 2012. An intertidal limpet species as a bioindicator:
505 Pollution effects reflected by shell characteristics. Ecol. Indic. 14, 178–183.
506 <https://doi.org/10.1016/j.ecolind.2011.07.015>
507

508 Palomares, M.L.D. and D. Pauly. Editors. 2019. SeaLifeBase. World Wide Web electronic
509 publication. www.sealifebase.org, version (04/2019)
510

511 Phillips, D.J.H., Rainbow, P.S., 1993. Biomonitoring of trace aquatic contaminants. Springer
512 Netherlands, Dordrecht, pp. 133–178. https://doi.org/10.1007/978-94-011-2122-4_6
513

514 Powell, B., Martens, M., 2005. A review of acid sulfate soil impacts, actions and policies that
515 impact on water quality in Great Barrier Reef catchments, including a case study on
516 remediation at East Trinity. *Mar. Pollut. Bull.* 51, 149–164.
517 <https://doi.org/10.1016/j.marpolbul.2004.10.047>
518

519 Proum, S., Harley, C.D., Steele, M., Marshall, D.J., 2017. Aerobic and behavioral flexibility
520 allow estuarine gastropods to flourish in rapidly changing and extreme pH conditions. *Mar.*
521 *Biol.* 164, 97. <https://doi.org/10.1007/s00227-017-3124-y>
522

523 Proum, S., Santos, J.H., Lim, L.H., Marshall, D.J., 2016. Metal accumulation in the tissues and
524 shells of *Indothais gradata* snails inhabiting soft and hard substrata in an acidified tropical
525 estuary (Brunei, South East Asia). *Reg. Stud. Mar. Sci.* 8, 487–497.
526 <https://doi.org/10.1016/j.rsma.2016.03.010>
527

528 Proum, S., Santos, J.H., Lim, L.H., Marshall, D.J., 2018. Tidal and seasonal variation in
529 carbonate chemistry, pH and salinity for a mineral-acidified tropical estuarine system. *Reg.*
530 *Stud. Mar. Sci.* 17, 17–27. <https://doi.org/10.1016/j.rsma.2017.11.004>
531

532 Rohlf, F.J., 1996. Morphometric spaces, shape components and the effects of linear
533 transformations, in: Marcus, L.F., Corti, M., Loy, A., Naylor, G.J.P., Slice, D.E. (Eds.),
534 *Advances in Morphometrics*. Springer US, Boston, MA, pp. 117–129.
535 https://doi.org/10.1007/978-1-4757-9083-2_11
536

537 Rohlf, F.J., Slice, D., 1990. Extensions of the Procrustes method for the optimal
538 superimposition of landmarks. *Syst. Biol.* 39, 40–59. <https://doi.org/10.2307/2992207>
539

540 Schönberg, C.H.L., Fang, J.K.H., Carreiro-Silva, M., Tribollet, A., Wisshak, M., 2017.
541 Bioerosion: the other ocean acidification problem. *ICES J. Mar. Sci.* 74, 895–925.
542 <https://doi.org/10.1093/icesjms/fsw254>
543

544 Spalding, M.D., Fox, H.E., Allen, G.R., Davidson, N., Ferdaña, Z.A., Finlayson, M., Halpern,
545 B.S., Jorge, M.A., Lombana, A., Lourie, S.A., Martin, K.D., Mcmanus, E., Molnar, J., Recchia,
546 C.A., Robertson, J., 2007. Marine ecoregions of the world: A bioregionalization of coastal and
547 shelf areas. *Bioscience*, 57, 573-583.
548

549 Underwood, A.J., 1979. The ecology of intertidal gastropods. *Adv. Mar. Biol.* 16, 111–210.
550 [https://doi.org/10.1016/S0065-2881\(08\)60293-x](https://doi.org/10.1016/S0065-2881(08)60293-x)
551

552 Urish, D.W., McKenna, T.E., 2004. Tidal effects on ground water discharge through a sandy
553 marine beach. *Ground Water* 42, 971–982. [https://doi.org/10.1111/j.1745-](https://doi.org/10.1111/j.1745-6584.2004.tb02636.x)
554 [6584.2004.tb02636.x](https://doi.org/10.1111/j.1745-6584.2004.tb02636.x)
555

556 Waska, H., Greskowiak, J., Ahrens, J., Beck, M., Ahmerkamp, S., Böning, P., Brumsack,
557 H.J., Degenhardt, J., Ehlert, C., Engelen, B., Grünenbaum, N., Holtappels, M., Pahnke, K.,
558 Marchant, H.K., Massmann, G., Meier, D., Schnetger, B., Schwalfenberg, K., Simon,
559 H., Vandieken, V., Zielinski, O., Dittmar, T. 2019. Spatial and temporal patterns of pore water
560 chemistry in the inter-tidal zone of a high energy beach. *Front. Marine. Sci.*
561 <https://doi.org/10.3389/fmars.2019.00154>
562

563 Zelditch, M.L, Swiderski, D.L., Sheets, H.D., 2012. Geometric morphometrics for biologists:
564 A primer. Elsevier Academic Press, London.
565

566 Zhai, W.-D., Zang, K.-P., Huo, C., Zheng, N., Xu, X.-M., 2015. Occurrence of aragonite
567 corrosive water in the North Yellow Sea, near the Yalu River estuary, during a summer flood.
568 *Estuar. Coast. Shelf Sci.* 166, 199–208. <https://doi.org/10.1016/j.ecss.2015.02.010>
569

570 Zhou, Q., Zhang, J., Fu, J., Shi, J., Jiang, G., 2008. Biomonitoring: an appealing tool for
571 assessment of metal pollution in the aquatic ecosystem. *Anal. Chim. Acta* 606, 135–150.
572 <https://doi.org/10.1016/j.aca.2007.11.018>
573

574

575

576

577

578

579

580

581

582 **Figure captions**

583 **Figure 1.** Physical map showing sampling sites and waterways in Brunei Darussalam (Borneo,
584 South East Asia). JPMC (Jerudong Park Medical Centre), 4°56'55'' N, 114°49'42''E; PJER
585 (Pantai Jerudong), 4°57'30'' N, 114°50'22''E; PUN (Punyit), 4° 58' 30.3996" N, 114° 50'
586 56.7996"E; E1 (Empire), 4°58'08'' N, 114°51'18''E; E2 (Empire), 4°58'05'' N,
587 114°51'20''E; E3 (Empire), 4°58'05'' N, 114°51'19''E; TP (Pantai Tungku), 4°58'13'' N,
588 114°52'00''E; UB (Universiti Brunei Darussalam), 4°59'07'' N, 114°53'58''E.

589 **Figure 2.** Shell erosion ranking in *Nerita chamaeleon* (apical view). A quadrant and seven
590 sectors based on the shell growth pattern were established from a line drawn between the
591 columella notch (b) and the apex (circled a). The apex is the oldest shell with the growing edge
592 (labelled c) in sector 7. Two depths (types) of erosion were scored, Type I is deep erosion to
593 the fine textured, grey/white layer and Type II is superficial erosion of the pigmented, ridged
594 layer under the periostracum. A score was based on the highest sector showing > 50% eroded
595 shell. Shell A shows no erosion with the periostracum intact to the apex, shell B shows a ruffled
596 periostracum covering > 50% of sector 6 (scores 5 for Type II) and shell C shows complete
597 Type I erosion in sector 5 and complete Type II erosion in sector 7.

598 **Figure 3.** Shell erosion ranking in *Planaxis sulcatus* (abapertural view). R1 (not shown), shell
599 whorls 1 and 2 (W1, W2) intact with fine ridges; R2, complete or incomplete ridges on W3;
600 R3, W3 completely worn but W4 mostly ridged; R4, W4 mostly to completely worn but body
601 whorl (WB) completely ridged; R5, WB eroded towards the right edge.

602 **Figure 4.** Upper and middle. pH and salinity at acidified sites E1, E2 and E3 and reference
603 sites, JMPC, PJER and PUN (n = 103). TP and UB were similar to other reference sites (pH
604 was 8.44 – 8.29 and salinity was 33.1 – 31 psu; n = 21). Bottom. Relationship between pH and
605 salinity at the acidified sites, with boxes showing conditions likely to cause calcite (Ca) or
606 aragonite (Ar) undersaturation (see Proum et al., 2018).

607 **Figure 5.** 2D-DCA plot (axes 1 vs. axis 2) for *P. sulcatus* shells from an acidified site (E2, blue
608 squares) and reference sites (UB, red crosses and TP, green crosses). TPS deformation grids
609 represent individuals located at both extremes of the x and y axes. The population from the
610 acidified site (E2, blue squares) overlaps weakly with reference populations. Correlations show
611 that DC1 is especially influenced by aperture shape and DC2 by shell height. ANOSIM results
612 were UB/E2, p = 0.01; UB/TP, p = 0.0177; E2/TP, p = 0.0001.

613 **Figure 6.** Eroded and total abapertural surface areas of *N. chamaeleon* shells from PUN
614 (reference, blue, n = 25) and E1 (acidified, red, n = 15), determined manually (A, B, C; mean
615 \pm 1 s.e.m). (D) Number of individuals with eroded (> 10%) and non-eroded shells.

616 **Figure 7.** Examples showing red-blue-white colour partitioning of shell surfaces, used in the
617 automated determination of percentage shell erosion (upper). Pixel numbers and percentage
618 erosion calculations are shown. A least squares linear regression relating manually and digitally
619 determined percentage erosion (lower).

620 **Figure 8.** *Nerita chamaeleon* shell erosion ranks (SER). (A) Box-Whisker plots and outliers of
621 SERs for three acidified (E1, E2, E2) and three reference (JMPC, PJER, PUN) sites using
622 combined Type I and II ranks (0-14). Different letters above plots indicate significant
623 differences between sites (see Table 1). (B) Snail frequencies at each site for Type I rank (0-
624 6).

625 **Figure 9.** *Planaxis sulcatus* shell erosion ranks (SER). (A) Box-Whisker plots and outliers of
626 SERs for three acidified (E1, E2, E2) and three reference (JMPC, PJER, PUN) sites for
627 apertural and abapertural surface ranks combined (2-10). Different letters above plots indicate
628 significant differences between sites (see Table 1). (B) Snail frequencies at each site (ranks 2-
629 5).

630

631